

5. R. W. Hornbeck, W. T. Rouleau, and F. S. Osterle, *Phys. Fluids*, 6, No. 11 (1963).
6. L. S. Galowin and V. A. Barker, ASME Paper No. HT-22 (1969).
7. L. S. Galowin, L. S. Fletcher, and M. J. Desantis, *J. Heat Transfer*, No. 2, 263 (1974).
8. L. S. Galowin, L. S. Fletcher, and M. J. Desantis, AIAA Paper No. 73-725 (1973).

COMPUTATION OF THE PRESSURE LOSS IN GAS FLOW THROUGH POROUS MATERIALS

V. D. Daragan, A. Yu. Kotov,
G. N. Mel'nikov, A. V. Pustogarov,
and V. I. Starshinov

UDC 532.546:537.527

The development of methods of designing the heat shield of high-heat-stressed elements of power plants, particularly plasmatrons, by blowing coolant through permeable structure elements requires a study, firstly, of the gas flow hydrodynamics in a porous material. The rise in the specific power of a plasmatron, and hence, the thermal loading of its elements, the use of blowing through a porous wall as a method of delivering the working body into the channel [1], result in the need to use blowing with high specific gas mass flow rates. The features of flows with high specific mass flow rates are the predominance of inertial pressure losses over the viscous losses, the rise in the pressure losses at the entrance and exit from the porous wall, the necessity to take account of compressibility in describing the flow in a porous medium. A rise in the mass flow rate through a wall can result in "choking" of the flow, i.e., in a mode when the mass flow rate will remain constant for a constant pressure in front of the wall, independently of the pressure change at the exit.

The flow in porous media with compressibility taken into account is inadequately investigated. The influence of compressibility on the flow as a function of the porous material characteristics and of the magnitude of the mass flow rate is analyzed in [2, 3] on a capillary model of a porous body. The presence of "choking" effects was experimentally confirmed in [4, 5]. The influence of material porosity on the "choking" was considered in [6]. However, actual porous materials are characterized by a complex pore space, a difference in pore and interpore passage sizes, convolutions of the pore channels, which constrain the application of an analysis based on a capillary model [2, 3].

The hydraulic drag of a porous wall can be determined from the expression [7]

$$\frac{P_2 - P_1}{L} = \xi \frac{2\rho v^2}{d}, \quad (1)$$

where ξ is the hydraulic drag coefficient; P_2 and P_1 , gas pressure at the entrance and exit from a porous wall of thickness L ; and v and d , characteristic velocity and geometric size. Selection of the characteristic parameters for a porous material is ambiguous. The filtration velocity $v_f = G/\rho F$ (G is the mass flow rate through a porous wall with cross-sectional area F at a normal velocity) or the mean velocity in the pores $v_p = v_f/\Pi$, where Π is the porosity, is taken as the characteristic velocity. The particle diameter d_{par} or the mean pore diameter d_p [7] is taken as the characteristic dimension. Since ξ is a function of not only the material structure but also the flow mode $\epsilon = f(Re)$, the results for different porous materials [7] is not extended successfully by means of (1). Flow deviation from the Darcy law occurs for values of Re substantially less than should have been expected on the basis of computations for models with channels with the characteristic dimensions d_{par} and d_p taken since the passage to the inertial flow mode is determined not only by the size of the pore channels but also by the shape, convolution, contractions, and expansions. Moreover, substantial errors are inherent to the very methods for determining the mean pore and particle size.

The two-term mode of writing the fluid motion equation

$$-\frac{dP}{dx} = \alpha w + \beta \rho v^2 \quad (2)$$

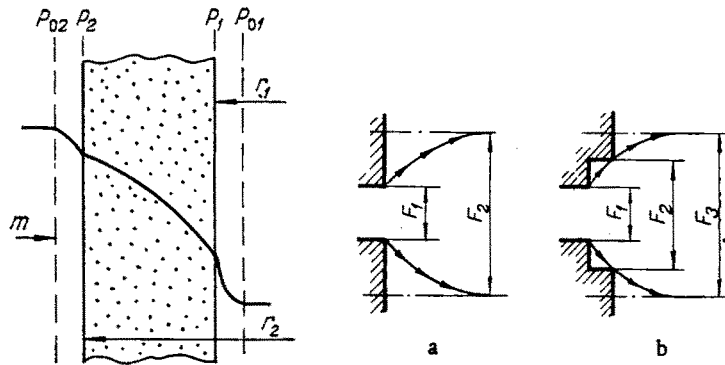


Fig. 1. Pressure losses on a porous wall and diagram of a one (a) and two-step (b) gas expansion at the exit from a porous body: a) $F_1 = f$, $F_2 = 1$; b) $F_1 = f$, $F_2 = \Pi$, $F_3 = 1$.

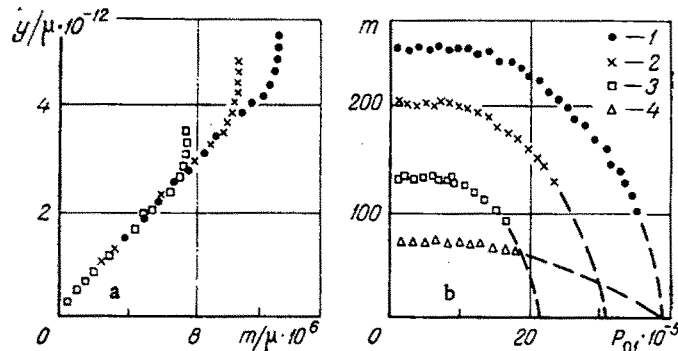


Fig. 2. Dependence $y/\mu = f(m/\mu)$ for air blown through a stainless steel bushing (a) and of specific mass flow rate of air m on the pressure in the exit tank (b) for a constant pressure in the entrance tank: 1) $P_{02} = 39.2 \cdot 10^5$ Pa; 2) 31.2; 3) 20.8; 4) 40; 1, 2, 3) $r_1 = 17 \cdot 10^{-3}$ m; $r_2 = 20 \cdot 10^{-3}$ m, $\Pi = 0.4$; 4) $r_1 = 10 \cdot 10^{-3}$ m; $r_2 = 20 \cdot 10^{-3}$ m, $\Pi = 0.42$; $y/\mu \cdot 10^{-12}$, m^{-2} ; $m/\mu \cdot 10^6$, m^{-1} ; m , $kg/m^2 \cdot sec$; $P_{01} \cdot 10^5$, Pa.

is used extensively to describe the flow in porous media. Use of the ratio β/α as the characteristic dimension permits obtaining one criterial dependence

$$\xi = \frac{2}{Re} + 2, \quad Re \sim f(\beta/\alpha) \quad (3)$$

for the hydraulic drag coefficients of any porous materials. It should be noted that dependence (3) has no essential practical value since an experimental determination of the coefficients α and β is necessary, and when known is already sufficient for the computation of the hydraulic drag.

The gas pressure loss in a porous medium is computed in this paper by using the coefficients α and β . They were experimentally determined in cylindrical specimens by means of the measured dependence of the pressure drop ΔP on the specific mass flow rate m by a graphic-analytic method using (1) converted to the form

$$(2P_2 - \Delta P) \Delta P / 2RTm\mu\Delta r = \alpha \frac{r_1}{\Delta r} \ln \left(\frac{r_2}{r_1} \right) + \beta \frac{r_1}{r_2} \frac{m}{\mu} \quad (4)$$

and later to

$$y/\mu = a + bm/\mu. \quad (5)$$

Here R is the gas constant and r_1 , r_2 , and Δr are, respectively, the inner and outer radii and the wall thickness. The quantity T was taken equal to the arithmetic mean value of the gas temperatures measured at the entrance and exit. The method of processing the experimental

data by means of the dependence $y/\mu = f(m/\mu)$ permits taking account of the change in viscosity during the change in the pressure level in the range of the modes to determine the drag coefficient with respect to m .

The experiment was conducted as follows. For given pressures in the entrance P_{02} and exit $P_{01} = P_{02}$ tanks (Fig. 1) the P_{01} is reduced while keeping P_{02} constant, which resulted in an increase in the mass flow rate through the wall. Neglecting the entrance and exit losses ($P_2 = P_{02}$, $P_1 = P_{01}$), the dependence $y/\mu = f(m/\mu)$ is constructed by means of the results of blowing, from which the values of α and β were determined. The range of the specific mass flow rates m to obtain dependence (5) in the experiment was 0.26–265 kg/m²·sec (air) for porous steel, for example.

Below a certain value of P_{01} the magnitude of the mass flow rate remains unchanged (Fig. 2) as the pressure drop $P_{02} - P_{01}$ grows ($P_{02} = \text{const}$), which results in a deviation of the dependence $y/\mu = f(m/\mu)$ from linear. This effect is associated with the build up of the speed of sound at the exit from the porous material, "choking" of the flow. Determining α and β in the nonlinear section is meaningless. To estimate the mode of a flow with "choking," it is necessary to know the porous material characteristic, such as the specific critical section

$$f = F_{\text{min}}/F, \quad (6)$$

where F_{min} is the least area formed by the holes for passage of the gas at the normal section velocity; F is the total area of the specimen normal section velocity. In the case of the capillary model of a porous body, it is assumed that $f = \Pi$, while for real porous powder materials $f < \Pi$. Both α and β and the value of f can be confidently determined by experiment only, e.g., by the method elucidated earlier. The flow mode when the specific mass flow rate m^* is already independent of the pressure P_{01} , i.e., a strictly horizontal section is obtained on the dependence $m = f(P_{01})$ (Fig. 2), is assured by the reduction of the pressure P_{01} for $P_{02} = \text{const}$. The presence of an extended passage to the horizontal section is a result of the pore-size distribution inherent to porous materials. This means that the "choking" mode is not determined by the single pressure at the exit P_{01} but by the domain of values of P_{01} . The horizontal section of the dependence corresponds to the passage to a flow with "choking" for the whole range of pore sizes.

The pressure at the exit

$$P_1^* = \sqrt{P_2^* - 2RT\Delta r [\alpha\mu (r_1/\Delta r) \ln(r_2/r_1) m + \beta (r_1/r_2) m^2]} \quad (7)$$

is determined by means of the values of m^* and $P_2^* = P_{02}$ (only neglecting the entrance losses) and the coefficients α and β obtained on the linear section of dependence (5). Later, the specific critical section

$$f = k^{-\frac{1}{2}} \left(\frac{2}{k+1} \right)^{-\frac{k+1}{2(k-1)}} \frac{m^*}{P_1^*} \sqrt{RT_0} \quad (8)$$

is found by means of P_1^* , the known m^* , and by considering the flow in the exit section sonic ($M = 1$), where k is the adiabatic index.

The mean value of f is obtained by obtaining P_1^* for different values of P_2^* and m^* .

It is possible to go from the specific critical section f to an estimation of the pressure loss at the exit, which is always higher than the entrance loss in connection with the lower gas pressure. The gas flow at the exit from a porous body can be considered as a sudden expansion after the section f in one or two steps. For single-step expansion (Fig. 1a), the area of the through section varies between f and 1.0, while for two-step, from f to Π and from Π to 1.0. The selection of the section $F_2 = \Pi$ is taken by analogy with the capillary model. The total pressure losses under a sudden expansion, neglecting friction on the wall, are expressed in terms of the gasdynamic functions [8]

$$\sigma = \frac{P_{01}}{P_1} = \frac{F_1}{F_2} \frac{q(\lambda_1)}{q(\lambda_2)}. \quad (9)$$

The value of λ_1 is considered known, but λ_2 is found from the relationship

$$z(\lambda_2) = z(\lambda_1) + \left(\frac{k+1}{2} \right)^{-\frac{1}{k-1}} \frac{1}{y(\lambda_1)} \left(\frac{F_2}{F_1} - 1 \right). \quad (10)$$

TABLE 1. Comparison of Computed and Experimental Data on Pressure Losses on a Porous Wall (Steel Kh18N10T, $r_1 = 17 \cdot 10^{-3}$ m, $\Delta r = 3 \cdot 10^{-3}$ m, $\alpha = 0.52 \cdot 10^{11}$ m $^{-2}$, $\beta = 0.26 \cdot 10^6$ m $^{-1}$, $f = 0.08$, $\Pi = 0.42$)

Mode	m , kg/m 2 sec	$P_{02} \cdot 10^{-5}$, Pa	$P_1 \cdot 10^{-5}$, Pa	$P_{01} \cdot 10^{-5}$, Pa one-step comp.	$P_{01} \cdot 10^{-5}$, Pa two-step comp.	$P_{01} \cdot 10^{-5}$, Pa (exp.)
1	135	20,6	7,5	4,35	5	5
2	200	30,9	12	7	8	8
3	253	38,8	14,5	8,5	9,8	10

TABLE 2. Dependence of the Total Pressure Loss at the Exit from a Porous Wall σ (Kh18N9T, $f = 0.08$, $\Pi = 0.42$) on the Velocity Coefficient λ_1

λ_1	0,1	0,2	0,3	0,4	0,5	0,6	0,7	0,8	0,9	1
σ	1	1	1	0,98	0,96	0,90	0,83	0,76	0,70	0,65

Here $q(\lambda)$, $z(\lambda)$, $y(\lambda)$ are gasdynamic functions; $\lambda = v/a_{cr}$, velocity coefficient; $q(\lambda) = \rho v / \rho_{cr} v_{cr}$, dimensionless stream density; $z(\lambda) = \lambda + 1/\lambda$; $y(\lambda) = q(\lambda)/\pi(\lambda)$; $\pi(\lambda) = P/P_0$, ratio of the pressure in the stream to the total pressure of an isentropic frozen gas. The values of the gasdynamic functions are taken from [8].

The flow mode with "choking" was considered in comparing the results of computations by means of the one- and two-step sudden expansion models with experiment. From the known $P_2 = P_{02}$, α , β , f , Π , and m^* for Kh18N9T steel walls, the P_1 was computed, and from tabulated values of $y(\lambda_1)$, $q(\lambda_1)$, $z(\lambda_1)$ for $\lambda = 1$ and given F_1 , F_2 and k , the $z(\lambda_2)$ and later the λ_2 were found from (10). The total pressure losses were determined from $q(\lambda_2)$ and expression (9). For a one-step expansion $\sigma = P_{01}/P_1 = 0.58$, and for a two-step $\sigma = 0.65$. The results presented in Table 1 to compare the computed and experimental data show that the two-step expansion model yields a more satisfactory agreement.

According to the estimate the total pressure losses for the flow modes with "choking" investigated are $\sim 17\%$ of the total pressure drop. For a flow without "choking" the values of the velocity coefficient λ_1 must be found in the section f by first determining P_1 from

$$m = \rho_1 v_1 f = a_{cr} \lambda_1 \rho_0 \varepsilon(\lambda_1) f, \quad \rho_0 = P_1 / RT_0. \quad (11)$$

The results of a computation of σ for a two-step model are represented in Table 2.

It follows from Table 1 that the total pressure losses at the exit for $\lambda_1 \leq 0.5$, and therefore, at the entrance can be neglected, i.e., it can be assumed that $P_2 = P_{02}$ and $P_1 = P_{01}$ in this range when determining the coefficients α and β . As estimates show, the quantity $\lambda = 0.5$ corresponds to ~ 0.92 m*.

The results of determining the viscous α and inertial β hydraulic drag coefficients of certain materials and information on their fabrication technology are represented in Table 3. An analysis of the results presented shows that the hydraulic characteristics of porous materials depend essentially on the fabrication technology and porosity, and require experimental determination in each specific case.

However, empirical dependences of α and β on the porosity, the size of the initial powder, etc. can be obtained within the limits of one fabrication technology to an accuracy sufficient for approximate computations of the pressure drop on a porous wall. The characteristic dimension β/α grows as the porosity and the size of the pore channels increase, and the role of the inertial term in (4) grows correspondingly.

The values of α and β characterize just the inner structure of the porous material. Their inconstancy indicates changes in the characteristics of the porous medium (deformation and chemical interaction) or the filtering fluid (condensation and evaporation). The coefficients α and β are practically independent of the temperature, although a change in the material structure does not set in (sintering, etc.). Constancy of the values of α and β is confirmed

TABLE 3. Values of the Hydraulic Drag Coefficients α and β for Materials of Different Porosity and Fabrication Technology

Material	Π	α, m^{-2}	β, m^{-1}	β/α	Fabrication technology
W	0,17	$5,90 \cdot 10^{13}$	$4,70 \cdot 10^7$	$0,08 \cdot 10^{-5}$	Hydrostatic stamping method, stamping pressure equals $(900-1000) \cdot 10^5$ Pa
—	0,25	$3,02 \cdot 10^{13}$	$8,47 \cdot 10^7$	$0,3 \cdot 10^{-5}$	$T_{sint} = 2300-2600^\circ K$, $d_{par} = (5-15) \cdot 10^{-6}$ m
W	0,28	$1,44 \cdot 10^{14}$	$4,80 \cdot 10^8$	$0,33 \cdot 10^{-5}$	Method of stamping with a low-melting core
—	0,50	$0,60 \cdot 10^{13}$	$4,60 \cdot 10^7$	$0,77 \cdot 10^{-5}$	Size of core fraction $(0,1-0,2) \cdot 10^{-3}$ m, $d_{par} = (5-15) \cdot 10^{-6}$ m
—	0,68	$0,25 \cdot 10^{12}$	$0,50 \cdot 10^7$	$2,00 \cdot 10^{-5}$	
W	0,64	$1,57 \cdot 10^{11}$	$1,86 \cdot 10^8$	$11,9 \cdot 10^{-5}$	Method of stamping with a low-melting core; size of core fraction $(8-12,5) \cdot 10^{-5}$ m
W	0,50	$4,43 \cdot 10^{11}$	$1,27 \cdot 10^7$	$2,86 \cdot 10^{-5}$	Method of deposition from the gas phase on to a copper wire carcass, removed by etching, $d_p = 0,5 \cdot 10^{-3}$ m
W	0,25	$1 \cdot 10^{13}$	—	—	Tungsten whiskers; whisker diameter $\equiv (25-30) \cdot 10^{-6}$ m
Kh18N9T	0,42	$5,2 \cdot 10^{10}$	$2,6 \cdot 10^5$	$0,5 \cdot 10^{-5}$	Hydrostatic stamping

in the purging of porous steel ($\Pi = 0.3-0.4$) by air for changes in the wall thickness in the range $(2-40) \cdot 10^{-3}$ m, the pressure at the entrance from 10^5 Pa to $150 \cdot 10^5$ Pa, and temperature from $200-870^\circ K$ [9, 10], and in porous tungsten W ($\Pi = 0.25$) for purging by Ar in the $300-700^\circ C$ temperature range.

The values of f for Kh18N9T steel in $3 \cdot 10^{-3}$ m ($\Pi = 0.40$) and 10^{-2} m ($\Pi = 0.42$) thick specimens were determined on the basis of the data presented in Fig. 2. The magnitudes of f were, respectively, 0.07 and 0.08, i.e., approximately one-fifth to one-sixth the value of Π .

An analysis of the influence of the pressure fluctuations in a channel, which reached 5% of the pressure level [11], and the changes in pressure along the channel axis, as well as the changes in the heat flux on the wall associated with the current and pressure fluctuations (and therefore, the gas temperature in the porous material) on the change in the coolant mass flow rate was performed according to (4) for the bushing of the interelectrode insert of a steel and tungsten plasmatron. It was assumed that the pressure P_{O_2} in the plenum did not vary. The results of the analysis are presented in Fig. 3. As the mean pressure level decreases in the channel, the changes in the mass flow rate caused by pressure deviation from the mean level diminish, and $\delta m = 0$ (curves 4 and 5) when the flow mode with "choking" is reached. The use of materials with the high energies α and β (tungsten, $\Pi = 0.2$) for the bushing of interelectrode inserts assures the stability of the mass flow rate through the wall for large pressure fluctuations in the channel. The influence of deviations in the mean gas temperature T_g on the change in specific mass flow rate through the wall for $P = \text{const}$ is more substantial for materials with a smaller characteristic dimension β/α , i.e., the large contribution of the viscous losses (curve 8).

Results of computing the pressure loss on the wall for a different specific mass flow rate of gas due to the pressure level in the channel (curves 1-4) and the mean gas temperature (5-7) are represented in Fig. 4. The horizontal sections of the curves correspond to flow modes with "choking." The dashed lines denote the computed dependences of the pressure drop at the wall without taking exit losses into account.

Therefore, a hydraulic computation of porous structural elements for high levels of the specific gas discharge (more than $50 \text{ kg/m}^2 \cdot \text{sec}$, air) should take into account the pressure loss at the entrance and exit from the porous wall, and the effect of "choking" of the flow. For porous materials with the characteristic dimension $\beta/\alpha > 10^{-5}$ m the contribution of the viscous drag for such mass flow rates is several percent of the inertial drag, and the computation of the pressure loss can be performed by means of the simplified expression (2)

$$-dP/dx = \beta \rho v^2. \quad (12)$$

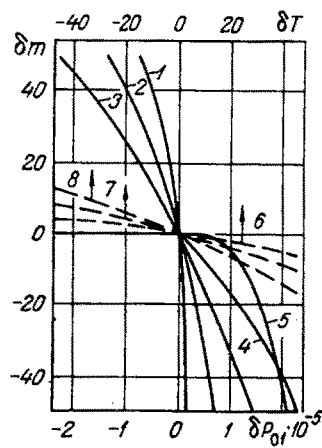


Fig. 3

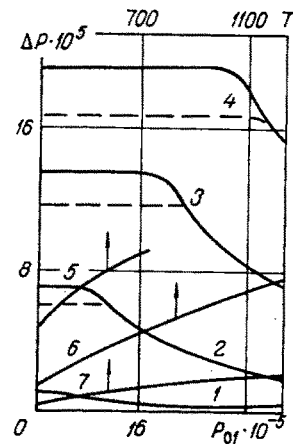


Fig. 4

Fig. 3. Relative change in the specific air mass flow rate for deviations in pressure at the exit (1-5) and the gas temperature (6-8) from the nominal values: 1) $P_{01} = 40 \cdot 10^5$ Pa; 2) $20 \cdot 10^5$; 3) $10 \cdot 10^5$; 4) $5 \cdot 10^5$; 5) $4 \cdot 10^5$; 6) $T_g = 400^\circ\text{K}$; 7) 1000; 8) 400. 1-7) Kh18N9T; 8) W; δm , %; δT , $^\circ\text{K}$; $\delta P_{01} \cdot 10^{-5}$, Pa.

Fig. 4. Dependence of the pressure drop on the wall on the pressure level in the channel (1-4) and the mean gas temperature (5-7): Kh18N9T, 1) $m = 10 \text{ kg/m}^2 \cdot \text{sec}$; 2) 100; 3) 200; 4) 500; 5) $P_{01} = 1 \cdot 10^5$ Pa; 6) $P_{01} = 40 \cdot 10^5$ Pa; 7) $P_{01} = 40 \cdot 10^5$ Pa; 5, 7) $m = 50 \text{ kg/m}^2 \cdot \text{sec}$; 6) $m = 100$; $\Delta P \cdot 10^5$ Pa; T , $^\circ\text{K}$; $P_{01} \cdot 10^{-5}$, Pa.

To take account of the nonisothermy of the flow in porous media, the combined solution of the thermal and hydrodynamic problems is necessary.

NOTATION

P , pressure, Pa; ρ , gas density, kg/m^3 ; v , flow velocity, m/sec; m , specific gas mass flow rate, $\text{kg/m}^2 \cdot \text{sec}$; R , gas constant, $\text{J/kg} \cdot \text{deg K}$; T , gas temperature, $^\circ\text{K}$; μ , viscosity, $\text{N} \cdot \text{sec/m}^2$; α , viscous hydraulic drag coefficient, m^{-2} ; β , inertial hydraulic drag coefficient, m^{-1} ; ξ , hydraulic drag coefficient; Π , material porosity; d_p , mean pore size, m; d_{par} , mean particle size of the porous material, m; Re , Reynolds number; β/α , characteristic dimension, m; F , area, m^2 .

LITERATURE CITED

1. A. B. Karabut, V. N. Korshunov, Yu. V. Kurochkin, A. V. Pustogarov, and M. N. Supronenko, "Electric arc generator with porous cooling of the interelectrode insert of 2-MW power," *Izv. Sib. Otd. Akad. Nauk SSSR, Ser. Tekh. Nauk*, No. 8, Issue 2 (1976).
2. G. Emanuel and J. P. Jones, "Compressible flow through a porous plate," *Int. J. Heat Mass Transfer*, 11, 827-836 (1968).
3. G. S. Beavers and E. M. Sparrow, "Compressible gas flow through a porous material," *Int. J. Heat Mass Transfer*, 14, 1855-1859 (1971).
4. I. E. Idel'chik, B. I. Voronin, I. V. Gordeev, and Yu. P. Matveev, "Experimental determination of the hydraulic characteristics of porous materials under high pressures," *Teploenergetika*, No. 1 (1973).
5. S. V. Belov, O. G. Kartuesov, and Yu. M. Novikov, "Conditions for the origination of a critical gas outflow from porous bodies," *Teploenergetika*, No. 2 (1976).
6. Yu. A. Lapshin, A. N. Piskunov, and V. K. Sheleg, "Investigation of the discharge characteristics of porous plates," in: *Intensification of the Energy and Material Transfer Processes in Porous Media at Low Temperatures* [in Russian], Minsk (1975).
7. S. V. Belov, *Porous Materials in Machine Construction* [in Russian], Mashinostroenie, Moscow (1976).

8. G. N. Abramovich, Applied Gas Dynamics [in Russian], Nauka, Moscow (1969).
9. D. B. Greenberg and E. Weger, "An investigation of the viscous and inertial coefficients for the flow of gases through porous sintered metals with high pressure gradients," Chem. Eng. Sci., 12, 8 (1960).
10. S. V. Belov, "Viscous and inertial coefficients of porous materials," Izv. Vyssh. Uchebn. Zaved., Mashinostr., No. 11 (1976).
11. L. V. Avdeev, N. M. Drachev, V. A. Kutsevalov, and B. V. Cheloznov, "Investigation of pressure fluctuations in a chamber, current and voltage intensities on the arc of a coaxial electric arc heater with external and internal magnetic fields," in: Sixth All-Union Conference on Low-Temperature Plasma Generators [in Russian], ILIM, Frunze (1974).

HEAT TRANSFER FOR A FREELY FLOWING FILM

V. I. Volodin and A. A. Mikhalevich

UDC 536.242:532.517

A numerical method has been applied to a turbulent-transport model to examine the cooling of a liquid film in a circular tube.

Most previous studies of film processes have been concerned with the heating of films or with heat transfer involving phase transitions [1-8], but the methods are limited in application to various flow conditions; e.g., laminar flow was envisaged in [4], while wave or turbulent flow was considered in [5-8].

We have made a numerical study of the cooling of a freely flowing convective film of liquid within a vertical tube with laminar and turbulent modes of flow; this is of some practical interest, since film condensation in power systems usually requires supercooling of the liquid in order to ensure normal pump operation. Turbulent transport is assumed, and satisfactory results are obtained for the entire flow range.

The steady-state axisymmetric free flow of the film on the internal surface of a vertical tube is considered subject to the condition that the mass flow rate and the physical parameters of the liquid are constant, while the longitudinal pressure gradient is zero. The following are the differential equations for conservation of momentum and energy:

$$\begin{aligned} \rho u \frac{\partial u}{\partial x} + \rho v \frac{\partial u}{\partial y} &= \frac{1}{r} \frac{\partial}{\partial y} \left(r \mu_{\text{eff}} \frac{\partial u}{\partial y} \right) + g(\rho_L - \rho_G), \\ \rho u \frac{\partial H}{\partial x} + \rho v \frac{\partial H}{\partial y} &= \frac{1}{r} \frac{\partial}{\partial y} \left[r \left(\frac{\mu_{\text{eff}}}{Pr_{\text{eff}}} \frac{\partial H}{\partial y} + \mu_{\text{eff}} u \frac{\partial u}{\partial y} \right) \right]. \end{aligned} \quad (1)$$

The total enthalpy is

$$H = c_p(T' - T) + \frac{u^2}{2}, \quad (2)$$

where T' is the inlet liquid temperature.

The effective viscosity and Prandtl number are given by:

$$\mu_{\text{eff}} = \mu + \mu_t, \quad Pr_{\text{eff}} = \frac{\mu_{\text{eff}}}{\frac{\mu}{Pr} + \frac{\mu_t}{Pr_t}}. \quad (3)$$

The value of Pr_t is taken as constant at 0.9 throughout the layer.

The turbulent viscosity is derived from Prandtl's mixing-length hypothesis:

$$\mu_t = \rho l^2 \left| \frac{\partial u}{\partial y} \right|. \quad (4)$$

Nuclear-Power Institute, Academy of Sciences of the Belorussian SSR, Minsk. Translated from *Inzhenerno-Fizicheskii Zhurnal*, Vol. 36, No. 5, pp. 795-799, May, 1979. Original article submitted May 11, 1978.